3 Biotech (2021) 11:102
https://doi.org/10.1007/s13205-021-02660-8

ORIGINAL ARTICLE

DNA photolyase from Antarctic marine bacterium *Rhodococcus* sp. NJ-530 can repair DNA damage caused by ultraviolet

Yingying He[1,2] · Changfeng Qu[2,3] · Liping Zhang[1,2] · Jinlai Miao[1,2,3]

Received: 30 September 2020 / Accepted: 13 January 2021 / Published online: 29 January 2021

Abstract

Marine bacterium *Rhodococcus* sp. NJ-530 has developed several ultraviolet (UV) adaptive characteristics for survival and growth in extreme Antarctic environment. *Rhodococcus* sp. NJ-530 DNA photolyase encoded by a 1146 bp photolyase-homologous region (*phr*) was identified in genome. Quantitative real-time PCR demonstrated that transcriptional levels of *phr* were highly up-regulated by ultraviolet-B (UV-B) radiation (90 μW·cm^{-2}) and increased to a maximum of 149.17-fold after exposure for 20 min. According to the results of SDS-PAGE and western blot, PHR was effectively induced by isopropyl-β-D-1-thiogalactopyranoside (IPTG) at the genetically engineered BL21(DE3)-pET-32a(+)-*phr* construct under the condition of 15 °C for 16 h and 37 °C for 4 h. In terms of in vivo activity, compared with a *phr*-defective *E. coli* strain, *phr*-transformed *E. coli* exhibited higher survival rate under high UV-B intensity of 90 μW·cm^{-2}. Meanwhile, the purified PHR, with blue light, presented obvious photorepair activity toward UV-induced DNA damage in vitro assays. To sum up, studying the mechanisms of *Rhodococcus* sp. NJ-530 photolyase is of great interest to understand the adaptation of polar bacteria to high UV radiation, and such data present important therapeutic value for further UV-induced human skin and genetic damage diseases.

Keywords Antarctica · *Rhodococcus* sp. NJ-530 · Photolyase · DNA damage · DNA repair · Photorepair

Introduction

Normally, ozone layer functions as an ultraviolet (UV, 280–400 nm) radiation barrier to absorb almost all ultraviolet-C (UV-C, 100–280 nm) radiation and approximately 90% of ultraviolet-B (UV-B, 280–315 nm) radiation (Hu and Adar 2017; Sinha and Hader 2002). It is unfortunate that the ozone layer has been severely damaged and depleted due to pollution and the use of fluoridated compounds, especially in Antarctica (Bais et al. 2015). The increased UV levels exert increasingly adverse effects on molecules such as DNA, protein and lipids in bacteria, fungi, plants, animals and even humans (Dahms and Lee 2010; Gill et al. 2015; Jans et al. 2005; Roldan-Arjona and Ariza 2009).

UV radiation has the oxidizing activity in triggering oxidative stress in organisms by generate reactive oxygen species (ROS), such as hydrogen peroxide (H_2O_2), hydroxyl radicals (·OH), superoxide anion radicals ($\cdot O_2^-$) and singlet oxygen ($^1O_2$) (Subedi et al. 2017). What is more, genotoxic UV light mainly damages organismic DNA in two ways: formation of cis-syn cyclobutane pyrimidine dimers (CPDs) and pyrimidine–pyrimidone (6–4) photoproducts [(6–4) PPs] (Kageyama and Waditee-Sirisattha 2019; Sancar 2004; Sinha and Hader 2002). CPDs are the major type of UV-induced dimers, and the spatial configuration of both photoproducts is altered compared to the DNA double-helix structure (Dehez et al. 2017). Unfortunately, if left unrepaired, the DNA damage may result in mutations or even cell

Supplementary Information The online version contains supplementary material available at https://doi.org/10.1007/s13205-021-02660-8.

✉ Changfeng Qu
cfqu@fio.org.cn

✉ Jinlai Miao
miaojinlai@fio.org.cn

1 Department of Specialty Medicine, School of Basic Medicine, Qingdao University, Qingdao 266071, China

2 Key Laboratory of Marine Eco-Environmental Science and Technology, First Institute of Oceanography, Ministry of Natural Resource, Qingdao 266061, China

3 Laboratory for Marine Drugs and Bioproducts, Qingdao Pilot National Laboratory for Marine Science and Technology, Qingdao 266237, China

death in organisms (Hader and Sinha 2005; Lee et al. 2018; Rastogi et al. 2010). In addition, UV-induced DNA damage causes a series of skin problems, such as inflammation, immunosuppression, and even skin cancer (Armstrong and Kricker 2001; Pfeifer and Besaratinia 2012). The protection of skin with traditional sunscreens is inherently prophylactic, while sunscreens containing DNA photolyase (EC 4.1.99.3) can repair DNA damage caused by UV-B (Berardesca et al. 2012). According to recent studies, topical use of photolyase is very effective in protecting human skin and serves as both a preventive measure and a method for treating UV-induced damage to human skin (Carducci et al. 2015; Laino et al. 2015; Megna et al. 2017; Purohit et al. 2016; Puviani et al. 2013; Stege et al. 2000). Photolyase, which belongs to CPF (cryptochrome (CRY) and photolyase family), specifically binds to CPDs or (6–4) PPs to repair UV-induced DNA damage using the energy from visible light photons (Stege et al. 2000). However, a single kind of photolyase cannot bind to both products. Thus, CPD photolyase can only repair CPDs, while 6–4 photolyase only repair (6–4) PPs.

The molecular mechanism of DNA photolyase has been extensively explored, but reports of photolyase in Antarctic microorganisms are still limited. To the best of our knowledge, Antarctic photolyases were found in bacteria *Pseudomonas*, *Hymenobacter* and *Sphingomonas* (Marizcurrena et al. 2019, 2017), unicellular green alga *Chlamydomonas* sp. ICE-L (Li et al. 2015), and several zooplankton (Isely et al. 2009; Malloy et al. 1997; Rocco et al. 2002). What is more, scientists also found photolyase gene in Antarctic bacterium *Hymenobacter nivis* P3^T and moss *Pohlia nutans*, but their functional characterization and verification had not been carried out yet (Li et al. 2019; Terashima et al. 2019). Therefore, in this study, the actinomycete *Rhodococcus* sp. NJ-530 from Antarctica was selected as experimental model to study DNA photolyase in view of extreme UV adaptability. We successfully cloned and expressed the photolyase-homologous region (PHR) from *Rhodococcus* sp. NJ-530 genome, which establishes a foundation for studying UV radiation response in certain *Rhodococcus* strains.

Materials and methods

Bacterial strain and culture method

Rhodococcus sp. NJ-530 was isolated from floating ice near the Zhongshan Research Station of Antarctica (69° S, 77° E) during China's 22nd Antarctic Expedition in 2001. The complete genome of *Rhodococcus* sp. NJ-530 was sequenced and submitted to National Center for Biotechnology Information (NCBI) website under the accession Number of NZ_CP034152.1. The sample was stored at the Key Laboratory of Marine Bioactive Substances, First Institute of Oceanography, Ministry of Natural Resources, China. Cultures were incubated in 2216E medium at 25 °C.

Bioinformatic analysis

The open-reading frame (ORF) and homology of *phr* were analyzed with ORF Finder and BLASTX, respectively, from NCBI website. Nucleotide sequence of *phr* was translated into a protein sequence (http://searchlauncher.bcm.tmc.edu/seq-util/Options/sixframe.html). Then, theoretical isoelectric point (pI) and molecular weight (Mw) of the photolyase were calculated using Compute pI/Mw tool in ExPASy (http://web.expasy.org/protparam). Predictprotein (https://www.predictprotein.org/) and Swiss-Model were used to predict its function and structure (Waterhouse et al. 2018). Phylogenetic tree was built using neighbor-joining method and evaluated using a bootstrap analysis method with 1000 replicates by MEGA 6.0 software.

phr cloning and plasmid constructs

EasyPure® Bacteria Genomic DNA Kit (TransGen Biotech, Beijing, China) was used to extracted *Rhodococcus* sp. NJ-530 genomic DNA. Specific primers for *phr* (Table 1) were designed to amplify *phr* with *EasyTaq*® DNA polymerase (TransGen Biotech, Beijing, China) using *Rhodococcus* sp. NJ-530 genomic DNA as the template. PCR procedure was as follows: 94 °C for 3 min, 35 cycles of 94 °C for 30 s, 58 °C for 30 s, and 72 °C for 90 s, and a final step of 10 min

Table 1 Primers used in *phr* cloning and expression

Primers	Sequence (5′-3′)
Primers for *phr* cloning	
phr-F	CGGACAGACGTTGGGT
phr-R	TCAGCCTTTGATCTCGC
Primers for *phr* transcriptional expression	
phr-qF	CGCAACTGGTGGACGGTGAC
phr-qR	CTTCAACGAGTGGACGGCCTTC
16S rRNA-qF	TGCGAGACCGTGAGGTGGAG
16S rRNA-qR	GCGATTACTAGCGACTCCGACTTC
GAPDH-qF	CGACGGCAGCCAGAACATCATC
GAPDH-qR	GCGTGGATCGTGGTCATCAGAC
recA-qF	CACCACCGTCATCTTCATCAACCAG
recA-qR	CGACGGCAGCCAGAACATCATC
Ldh-qF	GACCAACCTCGCCATCGGATTG
Ldh-qR	CGTGGGAAGGGACAGGCAAAC
rpoB-qF	GTCGTTCAAGGTGCTCCTCAAGG
rpoB-qR	TCGTCGCCGTCCGCCATC
PGK-qF	GCGAGACCAGCAAGGACGAAG
PGK-qR	ACGCCTGCTTACGGTGAACAAC

at 72 °C. The desired PCR products were then separated by electrophoresis in a 1.0% agarose gel and purified using an *EasyPure*® PCR Purification Kit (TransGen Biotech, China). After inserted into PMD19T vector, the purified *phr* was maintained in *Escherichia coli* strain DH5α and finally sequenced (Sangon, China) to confirm its correctness.

Quantitative real-time PCR analysis of *phr* expression

Rhodococcus sp. NJ-530 cells were cultured to exponential growth phase for the analysis of *phr* transcription levels. Three biological replicates of cells in exponential growth phase were irradiated with UV-B at intensities of 0, 30, and 90 μW·cm^{-2} for different culture times (0, 10, 20, 40, 90 and 150 min) to investigate how *phr* was expressed at the transcriptional level in response to UV radiation. Meanwhile, OD_{600} value in different UV-B conditions was measured to draw the growth curve. RNA, extracted by *TransZol* (TransGen Biotech, China) from 10 mL of cells, was observed by electrophoresis in a 1.0% agarose gel and detected with NanoVue (GE Healthcare) (He et al. 2019). cDNA was obtained from high quality RNA with *PrimeScript*™ RT reagent kit with gDNA Eraser (Perfect Real Time) (Takara, Dalian).

Quantitative real-time PCR (qRT-PCR) was performed with an ABI StepOnePlus™ Real-Time PCR System (Applied Biosystems, USA) and SYBR *Premix Ex Taq*™ II (TaKaRa Biotech Co., Dalian, China). Following conditions were used for qRT-PCR: 95 °C for 30 s, 40 cycles of 95 °C for 5 s, 58 °C for 11 s, and 72 °C for 30 s, and a final step of 5 min at 72 °C. Housekeeping genes of *16S ribosomal RNA (16S rRNA)*, *glyceraldehyde-3-phosphate dehydrogenase (GAPDH)*, *phosphoglycerate kinase (PGK)*, *recombinase A (recA)*, *L-lactate dehydrogenase (Ldh)*, and *DNA-directed RNA polymerase subunit beta (rpoB)* were selected as internal control genes. Gene-specific primers used for qRT-PCR are shown in Table 1. Then, experimental data were further analyzed using Ct ($2^{-\Delta\Delta CT}$) model (Livak and Schmittgen 2001). Meanwhile, Ct raw data outputs were analyzed on EXCEL-based program BestKeeper and with geNorm program.

Codon optimization analysis and plasmid constructs

The codon optimization analysis (amino acid sequence invariance) was performed on the basis of codon adaptation index (CAI), GC content, restriction sites and cis-acting elements. In addition, Trx and His tags were added to the optimized *phr* in following order: ATG-Trx-His, tag-KpnI-TEV, protease, site-*phr*-Stop, codon-HindIII (GenScript Biotech Corp, Nanjing, China). The final sequence containing *phr* was inserted into expression vector pET-32a(+), which was then transformed to *E. coli* BL21 (DE3) by screening and a positive clone with high expression was identified. The sequence of final constructed recombinant strain BL21(DE3)-pET-32a(+)-*phr* was verified again and then preserved for subsequent PHR expression.

PHR expression, purification and detection

BL21(DE3)-pET-32a(+)-*phr* was inoculated into a 1-L Erlenmeyer flask containing 300 mL of liquid LB medium and 100 μg·mL^{-1} ampicillin, followed by incubation at 37 °C with shaking at 220 rpm. When OD_{600} reached 0.6 ~ 0.8, isopropyl-β-D-1-thiogalactopyranoside (IPTG) was added to a final concentration of 0.5 mM, and the culture was incubated at 15 °C for 16 h or at 37 °C for 4 h with shaking at 150 rpm to induce PHR expression, after which cells were collected by centrifugation. BL21(DE3)-pET-32a(+) without IPTG was used as a control.

The collected bacterial cells were suspended in lysis buffer 1 (150 mM NaCl, 0.5 mM Phenylmethanesulfonyl fluoride and 25 mM Tris, pH 8.0), disrupted by ultrasonication (JY88-IIN, Ningbo Scientz Biotechnology, China), and then centrifuged at 12,000×*g* for 20 min at 4 °C. At this point, supernatant and cell sediments in cell lysate were collected. Cell sediments were resuspended with lysis buffer 2 (7 M guanidine hydrochloride, 50 mM Tris, 300 mM NaCl, 0.1% Triton X-100, pH 8.0), and then further purified with Ni–NTA resin (TaKaRa BIO INC., Beijing, China) to harvest PHR protein. After renatured via a dialysis bag of 25 kDa in dialysis solution (50 mM Tris, 300 mM NaCl, pH 8.0) at 4 °C, purified protein were further concentrated to reconstituted for functional analysis. Protein expression and detection were determined using Mass Spectrometry (MS) analysis (Sangon, China), SDS-PAGE and western blot. The primary antibody used for western blot was an anti-His antibody (GenScript Biotech Corp, Nanjing, China).

In vivo photorepairing activity of PHR

Depending on pretest, BL21(DE3)-pET-32a(+) and BL21(DE3)-pET-32a(+)-*phr* in logarithmic phase were 105 fold times diluted and then steaked on LB agar plates. Experimental groups consisted of BL21(DE3)-pET-32a(+)-*phr* irradiated with UV-B (90 μW·cm^{-2}) for 0, 1, 2, 5, 10, 20, or 30 min and then recovered under visible light (80 μmol·m^{-2} s^{-1}) for 30 min. Control groups consisted of BL21(DE3)-pET-32a(+) subjected to the same conditions. The two groups of Petri dishes were cultured at 37 °C overnight. Survival rate was based on the number of monoclonal colonies surviving in each group under UV-B irradiation compared with survival rate without UV-B exposure: survival rate (%) = $(N/N_{total}) \times 100\%$ (N: numbers of monoclonal colonies that survived under UV-B irradiation; N_{total}: numbers of monoclonal colonies without UV-B). Three parallel experiments were performed for each set of conditions.

In vitro photorepairing activity of PHR

An oligo $(dT)_{16}$ (′5-TTT TTT TTT TTT TTT T-3′) solution was exposed to 100 μW·cm^{-2} of UV-B lamps (Beijing Normal University, Beijing, China) for 9 h to obtain CPDs substrates. OD_{260} values for oligo $(dT)_{16}$ were measured at 0, 3, 5.5, 7.5 and 9 min. Meanwhile, repair buffer (50 mM Tris–HCl, 100 mM NaCl, 1 mM EDTA, 10% glycerol, and 1 mM dithiothreitol, pH 7.6) was prepared. In vitro photorepairing activity of PHR was tested (total 300 μL) by adding 1 μM purified PHR to prepared 200 μL repair buffer and 5 μM UV-oligo $(dT)_{16}$. The mixture was placed in the dark for 15 min, and then exposed to blue light (450 nm, 10 nm FWHM, 50 μmol·m^{-2} s^{-1}). OD_{260} value of the initial UV-oligo $(dT)_{16}$ and repair buffer was set as 0. Then, OD_{260} values were measured at 0, 2, 10, 40, 60, and 100 min to evaluate UV-induced DNA damage repair activity of the purified PHR. In the control group, purified PHR was replaced by bovine serum albumin (BSA) (Li et al. 2015; Mu et al. 2005).

Statistical analysis

The statistical tests of LSD were carried out in SPSS 19.0, and p values of < 0.05 were considered as being significant.

Results

Real-time PCR analysis of *phr* mRNA expression

After analyzed by Ct ($2^{-\Delta\Delta CT}$) model, EXCEL-based program BestKeeper and geNorm program, *16S rRNA*, *GAPDH*, *PGK* were finally suitable for normalization. Figure 1a exhibits the growth states of *Rhodococcus* sp. NJ-530 with (30 μW·cm^{-2} or 90 μW·cm^{-2}) or without UV-B irradiation. In contrast to normal condition, UV-B irradiation inhibited *Rhodococcus* sp. NJ-530 growth in a dose-dependent manner. As shown in Fig. 1b, the relative mRNA expression of *phr* in *Rhodococcus* sp. NJ-530 presented different variations in response to different UV-B stresses. Transcriptional expression level of *phr* gradually increased, reaching maximum values (28.48 and 149.17, respectively) at 40 min under 30 μW·cm^{-2} and 90 μW·cm^{-2} UV-B irradiation. In addition, during experimental period, *phr* was expressed at significantly higher levels in *Rhodococcus* sp. NJ-530 exposed to a stronger UV-B irradiation (90 μW·cm^{-2}) than a lower UV-B radiation (30 μW·cm^{-2}). The expression levels then decreased but remained in a state of upregulation.

phr cloning, bioinformatics analysis, and codon optimization

The 1146 bp length of *phr* predicted from the genome of *Rhodococcus* sp. NJ-530 was successfully amplified and verified with molecular techniques and then submitted to GenBank under accession number MH844561. *phr* sequence encoded a polypeptide of 381 amino acids (Supplementary Fig. 1). pI and Mw of the PHR were 5.97 and 43.06 kDa, respectively. Figure 2 depicts tertiary structure of PHR, where a DNA photolyase from *E. coli* was used as a template (Park et al. 1995). Phylogenetic tree of CPF (Supplementary Fig. 2) was divided into eight branches of CPD Class I PHR, CPD Class II PHR, CPD Class III PHR, Plant PHR2, (6–4) prokaryotic PHR, (6–4) eukaryotic PHR, DASH (Drosophila, Arabidopsis, Synechocystis, Homo) CRY, and Plant CRY. PHR of *Rhodococcus* sp. NJ-530 belongs to CPD Class I PHRs. Finally, the total number of base pairs in final modified *phr* (Supplementary Fig. 3) with tags was 1620,

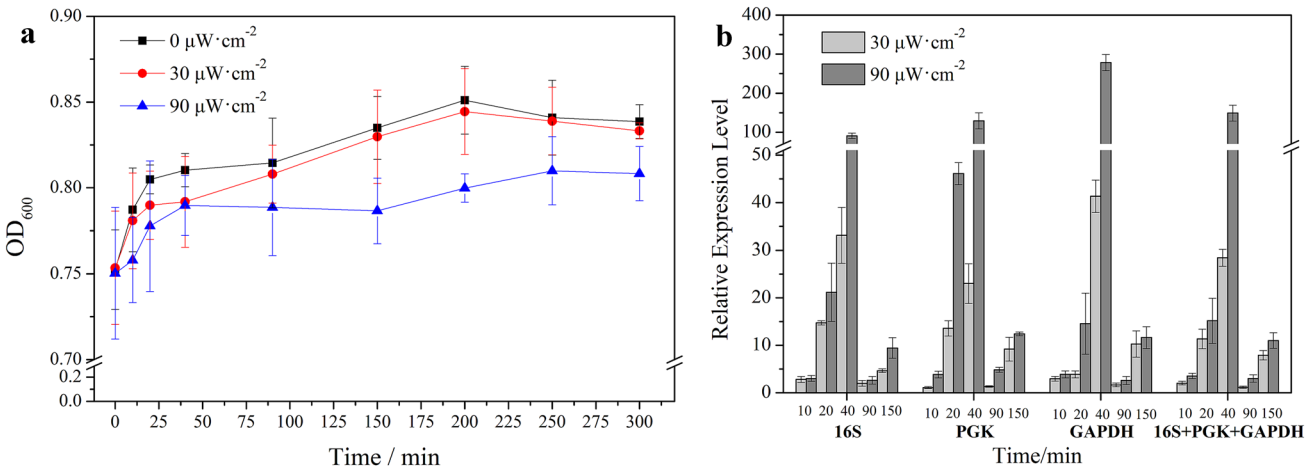

Fig. 1 Growth curve (**a**) and *phr* transcriptional expression levels (**b**) of *Rhodococcus* sp. NJ-530 under different UV-B radiation intensities

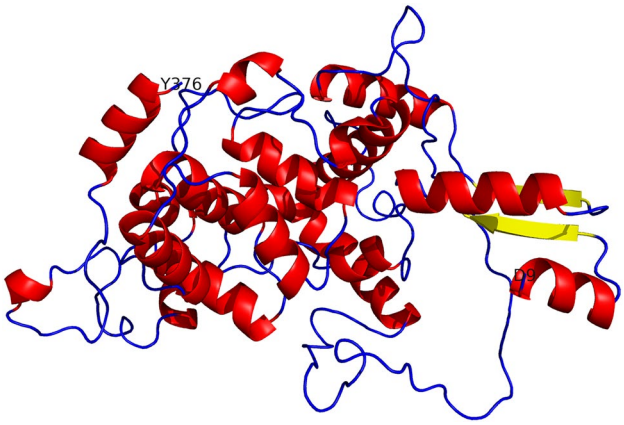

Fig. 2 Tertiary structure of PHR from *Rhodococcus* sp. NJ-530. Helix was shown in red, beta sheet in yellow, and others in blue

and the corresponding number of amino acids was 540. Predicted pI and Mw were 6.30 and 60.24 kDa.

Plasmid constructs, PHR expression, purification and in vivo photorepairing activity

Gratifyingly, as shown in Fig. 3a, b, BL21(DE3)-pET-32a(+)-*phr* was successfully induced to express photolyase protein in the sediments of cell lysate under incubation at 15 °C for 16 h and 37 °C for 4 h. Simultaneously, the size of target protein verified by SDS-PAGE and western blotting was consistent with the predicted. Furthermore, Fig. 3c demonstrates that after Ni–NTA resin purification, PHR was separated from protein mixture, and the 200 mM imidazole eluent showed a refined PHR product. What is more, MS analysis indicated that the coverage of purified PHR protein and target protein sequence was 27% (Supplementary Fig. 4).

In vivo photolyase activity assays of PHR are shown in Fig. 4. As UV-B irradiation time increased, the survival rates of both BL21(DE3)-pET-32a(+)-*phr* and BL21(DE3)-pET-32a(+) gradually decreased. In addition, UV-B exposure of 90 $\mu W \cdot cm^{-2}$ for more than 10 min was completely lethal for both groups of bacteria, with mortality reaching 100%. It is worth noting that the survival rate of BL21(DE3)-pET-32a(+)-*phr* was higher than that of BL21(DE3)-pET-32a(+) following UV-B irradiation for up to 5 min. These preliminary results confirmed that UV-B resistance of defective *E. coli* was increased by exogenous *phr* from *Rhodococcus* sp. NJ-530.

In vitro photorepairing activity of PHR

The results regarding in vitro photorepair activity of PHR expressed and purified from BL21(DE3)-pET-32a(+)-*phr* are shown in Fig. 5. In UV-oligo $(dT)_{16}$ prepare phase, Fig. 5a revealed that UV-B radiation for increasing times could decrease the absorbance value of oligo$(dT)_{16}$ at 260 nm from 1.21 to 0.58, which indicated that DNA damage resulted in forming CPDs. Figure 5b shows that after adding purified photolyase, damaged CPDs were largely repaired, as shown by OD_{260}, which increased to 0.134 at 10 min, and then gradually decreased, indicating a relatively good reparation.

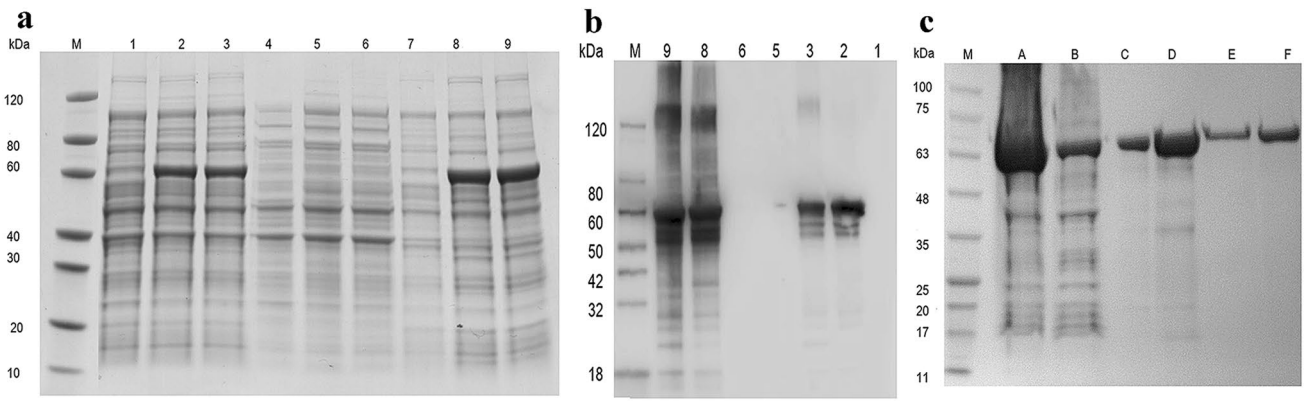

Fig. 3 SDS-PAGE (**a**) and western blot (**b**) analysis for total protein and SDS-PAGE (**c**) analysis for purified PHR expressed in BL21(DE3)-pET-32a(+)-*phr* (Lane M: protein marker; Lane 1: cell lysate of vector pET-32a without induction; Lane 2: cell lysate with induction for 16 h at 15 °C; Lane 3: cell lysate with induction for 4 h at 37 °C; Lane 4: supernatant of cell lysate of vector pET-32a without induction; Lane 5: supernatant of cell lysate with induction for 16 h at 15 °C; Lane 6: supernatant of cell lysate with induction for 4 h at 37 °C; Lane 7: sediments of cell lysate of vector pET-32a without induction; Lane 8: sediments of cell lysate with induction for 16 h at 15 °C; Lane 9: sediments of cell lysate with induction for 4 h at 37 °C; Lane A: unpurified protein; lane B: sample effluent; lane C: 20 mM imidazole eluate; lane D: 50 mM imidazole eluate; lane E: 500 mM imidazole eluate; Lane F: 200 mM imidazole eluate)

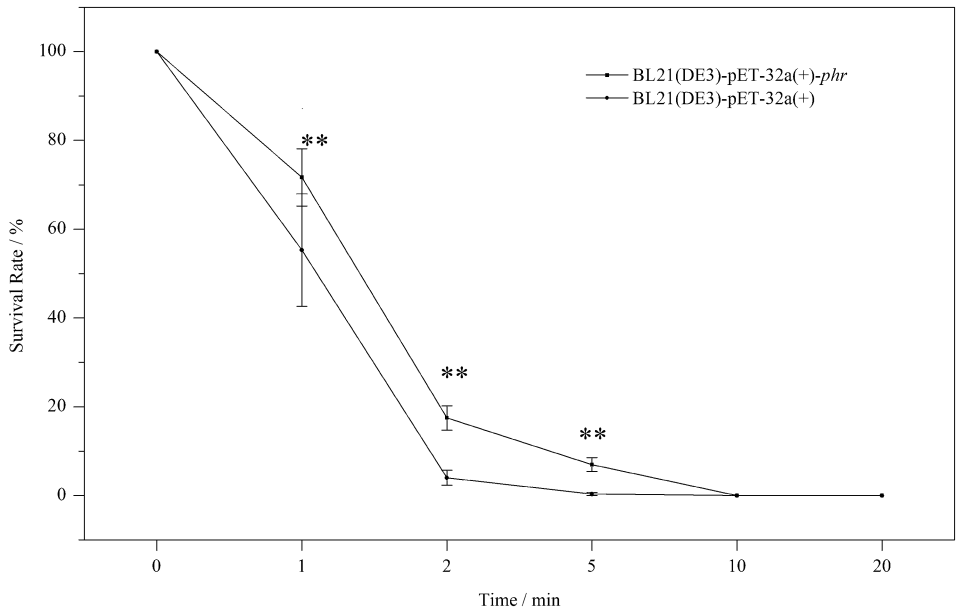

Fig. 4 Survival rate of *phr*-defective *E. coli* strain [BL21(DE3)-pET-32a(+)] and *phr*-transformed *E. coli* strain (BL21(DE3)-pET-32a(+)-*phr*). The method of LSD in SPSS 19.0, $P < 0.05$ for * and $P < 0.01$ for **

Discussion

Photolyase/cryptochrome genes have been identified in animals, plants, bacteria, fungi and human cells over the past few decades (Kobayashi et al. 1998; Landry et al. 1997; Li et al. 2015; Malhotra et al. 1994; Tagua et al. 2015; Todo et al. 1996). Since the first report of *E. coli* photolyase, bacterial photolyases have been extensively studied (Sancar et al. 1984). *Rhodococcus* sp. NJ-530 was isolated from Antarctic ice water and belongs to the actinomycetes. Bioinformatics analysis showed that PHR from *Rhodococcus* sp. NJ-530 has high similarity to *E. coli* photolyase. Considering that CPDs account for approximately 70% of DNA lesions (Bennett et al. 2003), studying CPD photolyase has become much more important in terms of practical significance and application value. This paper reports the cloning, expression, and in vivo and in vitro activity analyses of the unique photolyase gene *phr* from *Rhodococcus* sp. NJ-530, which have not previously been reported.

DNA repair by photolyases can be summarized as three photoinduced processes: photoinitiation, photoreduction, and photoreactivation (Kim and Sundin 2001; Zhang et al. 2017). The activity of photolyase must be stimulated by light, which implies an essential requirement for photoreceptors. CPD PHRs belong to three groups: Class I (mostly in unicellular organisms), Class II (unicellular and multicellular organisms), and Class III (plants) (Ozturk 2017). In this research, results showed PHR from *Rhodococcus* sp. NJ-530 belonged to CPD Class I PHR.

Photolyase plays an irreplaceable role in physiological adaptation mechanisms of *Rhodococcus* sp. NJ-530 to

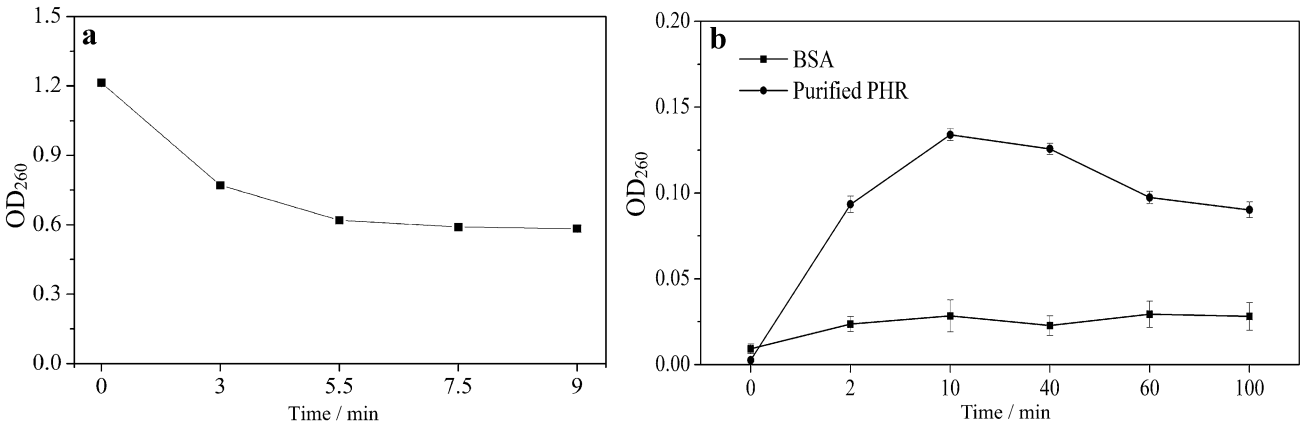

Fig. 5 Effect of purified PHR on photoreparation of UV-induced DNA damage. **a** The absorbance at 260 nm of oligo $(dT)_{16}$ irradiated with 100 $\mu W \cdot cm^{-2}$ UV-B. **b** CPDs photorepairing activity of PHR from *Rhodococcus* sp. NJ-530. BSA was set as control

adapt to high-intensity UV radiation in Antarctica. qRT-PCR analysis reflected the expression of *phr* in response to different intensities of UV-B radiation. Based on the results, transcriptional expression of *phr* was induced by stronger UV-B, which increased the expression of *phr* so that it was expressed at very high levels when exposed to high-intensity UV-B (90 $\mu W \cdot cm^{-2}$). Especially at 40 min, the relative expression level of *phr* was up to 149.17 times. Diurnal change in CPD photorepair activity, which is presumably regulated by transcript level of *phr*, may play an important role in minimizing growth inhibition due to UV-B irradiation. These research findings were consistent with previous results presented by other researchers (Kihara et al. 2004; Li et al. 2015; Takahashi et al. 2002). Compared with 40 min, *phr* expression level at 90 and 150 min were both decreased but still in an up-regulated level. The reason for decreasing may be related to *Rhodococcus* sp. NJ-530 passed logarithmic growth phase to stationary phase after 90 min (Fig. 1a).

Given the existence of codon usage bias in different organisms and tandem rare codons found in native genes that reduce the efficiency of translation or even disengage the translational machinery, a codon optimization analysis was performed to achieve expression of PHR in large quantities (Dever 2002). GC content and unfavorable peaks were optimized to prolong the half-life of mRNA. In addition, stem-loop structures were disrupted in consideration of impacting ribosomal binding and stability of mRNA. Finally, after all these attempts, PHR enzyme was expressed and purified from BL21(DE3)-pET-32a(+)-*phr* after induction with 0.5 mM IPTG at 15 °C for 16 h or 37 °C for 4 h.

Photolyase is important for the reparation of UV-induced gene damage and the prevention of further lethal biological effects. First, UV-resistance ability was detected in two *E. coli* strains, BL21(DE3)-pET-32a(+)-*phr* and BL21(DE3)-pET-32a(+). The survival rate of former strain was much higher than that of the latter, indicating that *phr* played important roles in UV radiation endurance in vivo. Finally, purified PHR was further used to explore photoreactivation activity of photolyase. Given that CPD photolyase can repair CPD damage induced by UV light, that UV-oligo $(dT)_{16}$ showed a trend of increasing over time in the presence of PHR, indicated that PHR exhibited effective photoreactivation activity. In addition, survival rate was significantly different at 1, 2 and 5 min, and increased by 0.4-, 3.25- and 19-folds, respectively. However, its enzyme activity was not maintained for long. Perhaps in vitro photoremediation reaction lacks a complete, recyclable electron-transfer mechanism (Liu et al. 2015; Zhang et al. 2017). All the findings in this study provide a theoretical reference for photolyase drug development in the hopes of preventing gene damage and even human skin cancer, which enriched the exploitation and utilization of Antarctic marine resources.

Conclusion

The prevention of UV-induced DNA damage and the ability to maintain stability and integrity of genetic material are essential for living organisms, particularly organisms living in areas with strong UVR. Therefore, we first isolated a strain of *Rhodococcus* sp. NJ-530 from Antarctic ice to explore the repair activity of photolyase. In this study, we expressed and purified PHR in *E. coli* (DE3). Simultaneously, in vitro and in vivo analysis showed considerable UV-induced DNA damage repair activities of purified PHR, which provides further insight supporting the use of photolyase in the treatment of photoimmunology and photocarcinogenesis.

Author contributions Conceptualization: CQ and JM; methodology: YH, CQ and JM; formal analysis and investigation: YH, LZ; writing—original draft preparation: YH; writing—review and editing: YH; funding acquisition: CQ and JM; supervision: CQ and JM.

Funding This study was funded by the National Key Research and Development Program of China (2018YFD0900705), the China Ocean Mineral Resources R&D Association (DY135-B2-14), the Natural Science Foundation of China (41576187), the Natural Science Foundation of Shandong (ZR2019BD023), Key Research and Development Program of Shandong Province (2018GHY115034, 2018GHY115039), Ningbo Public Service Platform for High-Value Utilization of Marine Biological Resources (NBHY-2017-P2), and Youth Fund Project of Shandong Natural Science Foundation (ZR2017QD008).

Compliance with ethical standards

Conflict of interest The authors declare that they have no conflict of interest.

Ethical approval This article does not contain any studies with human participants or animals performed by any of the authors.

References

Armstrong BK, Kricker A (2001) The epidemiology of UV induced skin cancer. J Photochem Photobiol B 63:8–18

Bais AF, McKenzie RL, Bernhard G, Aucamp PJ, Ilyas M, Madronich S, Tourpali K (2015) Ozone depletion and climate change: impacts on UV radiation. Photochem Photobiol Sci Off J Eur Photochem Assoc Eur Soc Photobiol 14:19–52. https://doi.org/10.1039/c4pp90032d

Bennett CJ, Webb M, Willer DO, Evans DH (2003) Genetic and phylogenetic characterization of the type II cyclobutane pyrimidine dimer photolyases encoded by Leporipoxviruses. Virology 315:10–19

Berardesca E, Bertona M, Altabas K, Altabas V, Emanuele E (2012) Reduced ultraviolet-induced DNA damage and apoptosis in human skin with topical application of a photolyase-containing DNA repair enzyme cream: clues to skin cancer prevention. Mol Med Rep 5:570–574. https://doi.org/10.3892/mmr.2011.673

Carducci M, Pavone PS, De Marco G, Lovati S, Altabas V, Altabas K, Emanuele E (2015) Comparative effects of sunscreens alone

vs sunscreens plus DNA repair enzymes in patients with actinic keratosis: clinical and molecular findings from a 6-month. Randomized Clin Study J Drugs Dermatol JDD 14:986–990

Dahms HU, Lee JS (2010) UV radiation in marine ectotherms: molecular effects and responses. Aquat Toxicol (Amsterdam, Netherlands) 97:3–14. https://doi.org/10.1016/j.aquatox.2009.12.002

Dehez F, Gattuso H, Bignon E, Morell C, Dumont E, Monari A (2017) Conformational polymorphism or structural invariance in DNA photoinduced lesions: implications for repair rates. Nucl Acids Res 45:3654–3662. https://doi.org/10.1093/nar/gkx148

Dever TE (2002) Gene-specific regulation by general translation factors. Cell 108:545–556

Gill SS, Anjum NA, Gill R, Jha M, Tuteja N (2015) DNA damage and repair in plants under ultraviolet and ionizing radiations. Sci World J 2015:250158. https://doi.org/10.1155/2015/250158

Hader DP, Sinha RP (2005) Solar ultraviolet radiation-induced DNA damage in aquatic organisms: potential environmental impact. Mutat Res 571:221–233. https://doi.org/10.1016/j.mrfmmm.2004.11.017

He Y et al (2019) Molecular cloning and functional analysis of a Delta(12)-fatty acid desaturase from the Antarctic microalga *Chlamydomonas* sp. ICE-L 3 Biotech 9:328. https://doi.org/10.1007/s13205-019-1858-6

Hu J, Adar S (2017) The cartography of UV-induced DNA damage formation and DNA repair. Photochem Photobiol 93:199–206. https://doi.org/10.1111/php.12668

Isely N, Lamare M, Marshall C, Barker M (2009) Expression of the DNA repair enzyme, photolyase, in developmental tissues and larvae, and in response to ambient UV-R in the Antarctic sea urchin *Sterechinus neumayeri*. Photochem photobiol 85:1168–1176. https://doi.org/10.1111/j.1751-1097.2009.00566.x

Jans J et al (2005) Powerful skin cancer protection by a CPD-photolyase transgene. Curr Biol CB 15:105–115. https://doi.org/10.1016/j.cub.2005.01.001

Kageyama H, Waditee-Sirisattha R (2019) Antioxidative, anti-inflammatory, and anti-aging properties of mycosporine-like amino acids: molecular and cellular mechanisms in the protection of skin-aging. Mar Drugs. https://doi.org/10.3390/md17040222

Kihara J, Moriwaki A, Matsuo N, Arase S, Honda Y (2004) Cloning, functional characterization, and near-ultraviolet radiation-enhanced expression of a photolyase gene (PHR1) from the phytopathogenic fungus *Bipolaris oryzae*. Curr Genet 46:37–46. https://doi.org/10.1007/s00294-004-0507-7

Kim JJ, Sundin GW (2001) Construction and analysis of photolyase mutants of Pseudomonas aeruginosa and Pseudomonas syringae: contribution of photoreactivation, nucleotide excision repair, and mutagenic DNA repair to cell survival and mutability following exposure to UV-B radiation. Appl Environ Microbiol 67:1405–1411. https://doi.org/10.1128/aem.67.4.1405-1411.2001

Kobayashi K, Kanno S, Smit B, van der Horst GT, Takao M, Yasui A (1998) Characterization of photolyase/blue-light receptor homologs in mouse and human cells. Nucl Acids Res 26:5086–5092

Laino L, Elia F, Desiderio F, Scarabello A, Sperduti I, Cota C, DiCarlo A (2015) The efficacy of a photolyase-based device on the cancerization field: a clinical and thermographic study. J Exper Clin Cancer Res CR 34:84. https://doi.org/10.1186/s13046-015-0203-0

Landry LG, Stapleton AE, Lim J, Hoffman P, Hays JB, Walbot V, Last RL (1997) An Arabidopsis photolyase mutant is hypersensitive to ultraviolet-B radiation. Proc Natl Acad Sci USA 94:328–332

Lee SJ, Lee MR, Kim S, Kim JC, Park SE, Shin TY, Kim JS (2018) Conidiogenesis-related DNA photolyase gene in *Beauveria bassiana*. J Invertebr Pathol 153:85–91. https://doi.org/10.1016/j.jip.2018.02.013

Li C et al (2015) Cyclobutane pyrimidine dimers photolyase from extremophilic microalga: remarkable UVB resistance and efficient DNA damage repair. Mutat Res 773:37–42. https://doi.org/10.1016/j.mrfmmm.2014.07.010

Li C, Liu S, Zhang W, Chen K, Zhang P (2019) Transcriptional profiling and physiological analysis reveal the critical roles of ROS-scavenging system in the Antarctic moss *Pohlia nutans* under Ultraviolet-B radiation. Plant Physiol Biochem PPB 134:113–122. https://doi.org/10.1016/j.plaphy.2018.10.034

Liu Z, Wang L, Zhong D (2015) Dynamics and mechanisms of DNA repair by photolyase. Phys Chem Chem Phys 17:11933–11949. https://doi.org/10.1039/c4cp05286b

Livak KJ, Schmittgen TD (2001) Analysis of relative gene expression data using real-time quantitative PCR and the 2(-Delta Delta C(T)). Method Methods 25:402–408. https://doi.org/10.1006/meth.2001.1262

Malhotra K, Kim ST, Sancar A (1994) Characterization of a medium wavelength type DNA photolyase: purification and properties of photolyase from *Bacillus firmus*. Biochemistry 33:8712–8718

Malloy KD, Holman MA, Mitchell D, Detrich HW 3rd (1997) Solar UVB-induced DNA damage and photoenzymatic DNA repair in Antarctic zooplankton. Proc Natl Acad Sci USA 94:1258–1263. https://doi.org/10.1073/pnas.94.4.1258

Marizcurrena JJ, Morel MA, Brana V, Morales D, Martinez-Lopez W, Castro-Sowinski S (2017) Searching for novel photolyases in UVC-resistant Antarctic bacteria. Extremophiles 21:409–418. https://doi.org/10.1007/s00792-016-0914-y

Marizcurrena JJ, Martinez-Lopez W, Ma H, Lamparter T, Castro-Sowinski S (2019) A highly efficient and cost-effective recombinant production of a bacterial photolyase from the Antarctic isolate *Hymenobacter* sp. UV11. Extremophiles 23:49–57. https://doi.org/10.1007/s00792-018-1059-y

Megna M, Lembo S, Balato N, Monfrecola G (2017) "Active" photoprotection: sunscreens with DNA repair enzymes Giornale italiano di dermatologia e venereologia : organo ufficiale. Societa italiana di dermatologia e sifilografia 152:302–307. https://doi.org/10.23736/s0392-0488.17.05567-5

Mu W, Zhang D, Xu L, Luo Z, Wang Y (2005) Activity assay of His-tagged *E. coli* DNA photolyase by RP-HPLC and SE-HPLC. J Biochem Biophys Methods 63:111–124. https://doi.org/10.1016/j.jbbm.2005.03.005

Ozturk N (2017) Phylogenetic and functional classification of the photolyase/cryptochrome family. Photochem Photobiol 93:104–111. https://doi.org/10.1111/php.12676

Park HW, Kim ST, Sancar A, Deisenhofer J (1995) Crystal structure of DNA photolyase from *Escherichia coli*. Science 268:1866–1872

Pfeifer GP, Besaratinia A (2012) UV wavelength-dependent DNA damage and human non-melanoma and melanoma skin cancer. Photochem Photobiol Sci Off J Eur Photochem Assoc Eur Soc Photobiol 11:90–97. https://doi.org/10.1039/c1pp05144j

Purohit NK, Robu M, Shah RG, Geacintov NE, Shah GM (2016) Characterization of the interactions of PARP-1 with UV-damaged DNA in vivo and in vitro. Sci Rep 6:19020. https://doi.org/10.1038/srep19020

Puviani M, Barcella A, Milani M (2013) Efficacy of a photolyase-based device in the treatment of cancerization field in patients with actinic keratosis and non-melanoma skin cancer Giornale italiano di dermatologia e venereologia : organo ufficiale. Societa italiana di dermatologia e sifilografia 148:693–698

Rastogi RP, Richa KA, Tyagi MB, Sinha RP (2010) Molecular mechanisms of ultraviolet radiation-induced DNA damage and repair. J Nucl Acids 1:592980. https://doi.org/10.4061/2010/592980

Rocco V, Oppezzo O, Pizarro R, Sommaruga R, Ferraro M, Zagarese H (2002) Ultraviolet damage and counteracting mechanisms in the freshwater copepod *Boeckella poppei* from the Antarctic

Peninsula. Limnol Oceanogr 47:829–836. https://doi.org/10.4319/lo.2002.47.3.0829

Roldan-Arjona T, Ariza RR (2009) Repair and tolerance of oxidative DNA damage in plants. Mutat Res 681:169–179. https://doi.org/10.1016/j.mrrev.2008.07.003

Sancar A (2004) Photolyase and cryptochrome blue-light photoreceptors. Adv Protein Chem 69:73–100. https://doi.org/10.1016/s0065-3233(04)69003-6

Sancar GB, Smith FW, Lorence MC, Rupert CS, Sancar A (1984) Sequences of the *Escherichia coli* photolyase gene and protein. J Biol Chem 259:6033–6038

Sinha RP, Hader DP (2002) UV-induced DNA damage and repair: a review. Photochem Photobiol Sci Off J Eur Photochem Assoc Eur Soc Photobiol 1:225–236

Stege H, Roza L, Vink AA, Grewe M, Ruzicka T, Grether-Beck S, Krutmann J (2000) Enzyme plus light therapy to repair DNA damage in ultraviolet-B-irradiated human skin. Proc Natl Acad Sci USA 97:1790–1795. https://doi.org/10.1073/pnas.030528897

Subedi L, Lee TH, Wahedi HM, Baek SH, Kim SY (2017) Resveratrol-enriched rice attenuates UVB-ROS-induced skin aging via down-regulation of inflammatory cascades. Oxid Med Cell Longev. https://doi.org/10.1155/2017/8379539

Tagua VG et al (2015) Fungal cryptochrome with DNA repair activity reveals an early stage in cryptochrome evolution. Proc Natl Acad Sci USA 112:15130–15135. https://doi.org/10.1073/pnas.1514637112

Takahashi S, Nakajima N, Saji H, Kondo N (2002) Diurnal change of cucumber CPD photolyase gene (CsPHR) expression and its physiological role in growth under UV-B irradiation. Plant Cell Physiol 43:342–349. https://doi.org/10.1093/pcp/pcf038

Terashima M, Ohashi K, Takasuka TE, Kojima H, Fukui M (2019) Antarctic heterotrophic bacterium Hymenobacter nivis P3(T) displays light-enhanced growth and expresses putative photoactive proteins. Environ Microbiol Rep 11:227–235. https://doi.org/10.1111/1758-2229.12702

Todo T et al (1996) Similarity among the Drosophila (6–4) photolyase, a human photolyase homolog, and the DNA photolyase-blue-light photoreceptor family. Science 272:109–112

Waterhouse A et al (2018) SWISS-MODEL: homology modelling of protein structures and complexes. Nucleic Acids Res 46:W296-w303. https://doi.org/10.1093/nar/gky427

Zhang M, Wang L, Zhong D (2017) Photolyase: Dynamics and electron-transfer mechanisms of DNA repair. Arch Biochem Biophys 632:158–174. https://doi.org/10.1016/j.abb.2017.08.007